Direct Time-Resolved Infrared Measurement of Electron Injection in Dye-Sensitized Titanium Dioxide Films

Todd A. Heimer[†] and Edwin J. Heilweil*

Optical Technology Division, Room B208, Building 221, National Institute of Standards and Technology, Gaithersburg, Maryland 20899

Received: August 6, 1997; In Final Form: October 2, 1997[⊗]

Time-resolved infrared (IR) spectroscopy in the 6 μm region was employed to study the excited-state properties of [Ru(4,4′-$(COOCH_2CH_3)_2$-2,2′-bipyridine)(2,2′-bipyridine$)_2$]$^{+2}$ and [Ru(4,4′-$(COOCH_2CH_3)_2$-2,2′-bipyridine)-(4,4′-$(CH_3)_2$-2,2′-bipyridine$)_2$]$^{+2}$ in solution and anchored to nanostructured thin films of TiO_2 and ZrO_2. Excited-state spectra reveal a shift in the ν(C═O) of the ester groups for the free molecules in solution as well as attached to insulating ZrO_2 substrates. For these molecules attached to TiO_2 semiconductor films, a transient absorption appears that is attributed to electrons injected into TiO_2. This absorption appears within the instrumental time resolution (ca. 30 ps) yielding an approximate 20 ps upper limit time constant for electron transfer from the sensitizer excited state to TiO_2.

Introduction

Since the development of highly efficient solar energy devices based on sensitization of wide bandgap semiconductors, interest in the processes occurring at the molecular dye/semiconductor interface has increased tremendously. Knowledge of electron-transfer rates in sensitized molecular photovoltaic devices is important because competition between excited-state decay, interfacial electron injection, and recombination rates determines the quantum yield of electrons transferred into the semiconductor and the overall photon-to-current conversion efficiency. Information on injection rates and their controlling factors is essential for further development of such devices, but direct measurement of these injection rates is an issue that remains unresolved.

Numerous studies involving photoluminescence[1] and transient visible absorbance measurements[2] at sensitizer/semiconductor interfaces have been published. However, few reports of mid-infrared measurements at the interface are known.[15] For metal complexes containing C═O or CN^- functionalities, this technique is particularly useful because the stretching vibrations have high oscillator strengths that give rise to strong signals in the IR region.[3,4] Further, the sensitivity of the vibrations to changes in molecular and electronic structure is well established.[3,4] For charge-transfer compounds, electronic excitation with visible light generally produces significant changes in electron density within the molecule, which can produce intense transient infrared absorption signals. For example, many time-resolved infrared (TRIR) studies have focused on metal-to-ligand charge transfer (MLCT) excited states of compounds with carbonyl or cyano ligands bound directly to the metal centers. Interpretation of excited-state spectra allows determination of charge localization in the excited state,[3a] photoinduced electron-transfer rates,[3b] or identification of intermediate states and products of photoinitiated reactions.[4]

Step-scan FTIR has recently been used to examine the excited state of [Ru(4,4′-$(COOCH_2CH_3)_2$-2,2′-bipyridine)(2,2′-bipyridine$)_2$]$^{2+}$, abbreviated [Ru(dceb)$(bpy)_2$]$^{2+}$, in acetonitrile solution.[5] The carbonyl group attached to the bipyridine ligand proved to be a strong indicator of electron density changes in the MLCT excited state. With ~20 ns time resolution, the ν(C═O) vibration at 1731 cm^{-1} shifted 26 cm^{-1} to lower energy following visible excitation, revealing that the excited triplet electron is localized on the ester-bearing ligand. This work clearly demonstrates the usefulness of TRIR in examining this class of compounds. Our intent was to expand on this work using ultrafast TRIR techniques to directly measure electron injection rates from sensitizers such as [Ru(dceb)$(bpy)_2$]$^{2+}$ to nanocrystalline TiO_2 semiconductor substrates.

Several research groups have measured electron injection rates for sensitized TiO_2 using time-resolved photoluminescence (TRPL).[1] Using this indirect method, the injection rate is calculated from the difference in $1/\tau$ (where τ is the sensitizer excited-state lifetime) on a semiconductor surface and on an insulating substrate where electron injection does not occur. The method assumes that the difference in lifetimes on the insulating and semiconducting surfaces is due solely to electron injection, which is difficult to establish. Further, the observed kinetics are complex, deviating significantly from exponential behavior and often requiring several fitting parameters.[1] Time constants obtained by this method vary widely: <7 ps for [Ru$(dcb)_2$-$(H_2O)_2$]$^{2+}$, (where dcb = 2,2′-bipyridyl-4,4′-dicarboxylate), 172 ps for the trinuclear compound Ru$(dcb)_2$-[CN-Ru$(bpy)_2$(CN)]$_2$, and 5 ns for [Ru$(dcb)_2(bpy)_2$]$^{2+}$.[1,6]

Recently, Durrant and co-workers[6] reported results from subpicosecond transient absorption measurements of the electron injection rate for Ru$(dcb)_2(NCS)_2/TiO_2$. This was also an indirect measurement, as the measured transient arises from the oxidized Ru^{III} cation. This species is formed primarily through electron injection but also appears if impurities, solvent, or other species present are reduced by the dye excited state. In addition, interpretation of the extracted kinetic rates is complicated by competing absorption of the Ru^{II} excited state (Ru^{II}*) . At the wavelength explored for kinetic measurements (750 nm), light absorption by Ru^{II}* contributes roughly 50% of the total signal. This presents a particular difficulty with subpicosecond measurements, as the Ru^{II}* T_1 state is formed in hundreds of femtoseconds for the related [Ru$(2,2'$-bipyridine$)_3$]$^{2+}$ molecule[7] and is expected to be similar for Ru$(dcb)_2(NCS)_2$.

To our knowledge, only one report exists of *direct* measurement of electron injection rates from ruthenium polypyridyl sensitizers to semiconductors. Kamat and co-workers time resolved the appearance of electrons in sensitized SnO_2 and ZnO by the growth of a microwave absorption feature.[8] The growth

[†] NRC/NIST Postdoctoral Research Associate.

[⊗] Abstract published in *Advance ACS Abstracts,* December 1, 1997.

S1089-5647(97)02560-1

kinetics agreed well with the fast component of a biexponential luminescence decay. Unfortunately, the time resolution of the microwave absorption experiment was limited to 3.5 ns, and weak signals prevented analysis of the injection rate for sensitized TiO_2.

In this Letter, we present the results of picosecond TRIR studies conducted in the 6 μm region applied to Ru sensitizers in solution and at ZrO_2 and TiO_2 interfaces. This experiment allows one to examine the nature of the surface-anchored MLCT excited state as well as to directly measure the rate of electron injection from the sensitizer excited state to TiO_2. In addition, the performance of an infrared HgCdTe array detector for TRIR spectroscopy is compared to 6 μm probe light upconversion into the visible region using CCD detection.

Experimental Section

Sensitizer Preparation. 4,4′-$(COOCH_2CH_3)_2$-2,2′-bipyridine (dceb) was prepared from commercially available 4,4′-$(COOH)_2$-2,2′-bipyridine (Aldrich)[9] by the method of Maerker and Case.[10] The ligands 2,2′-bipyridine (bpy) and 4,4′-$(CH_3)_2$-2,2′-bipyridine (dmb) were used as obtained from Aldrich. Standard procedures for the preparation of ruthenium tris-chelates from $RuCl_3$ hydrate (Aldrich) were followed,[11] and products were purified by recrystalization from dichloromethane/diethyl ether.[12] Dichloromethane (DCM) was dried over molecular sieves and filtered prior to use in synthesis or spectroscopy.

Sample Preparation. Transparent TiO_2 and ZrO_2 films were prepared from colloidal solutions[12] and deposited on the unpolished side of one-side polished CaF_2 25 mm diameter, 3 mm thick windows (International Crystal Laboratories).[9] Film adhesion to the rough surface is acceptable, transmittance in the mid-IR is >60%, and light scattering is minimal when the window is assembled in a cell filled with solution. Sensitizers were anchored to TiO_2 or ZrO_2 surfaces by soaking in $\sim 5 \times 10^{-3}$ mol/L DCM solutions for 24 h. For solution experiments, sensitizers were dissolved in DCM at a concentration of $(3-5) \times 10^{-3}$ mol/L to give optical density (OD) of 0.5−0.8 for the 1731 cm^{-1} ester CO stretch in a 2.5 mm path length CaF_2 windowed cell. For surface-anchored studies, one or both windows of the cell were replaced with a sensitized TiO_2 or ZrO_2 coated window, with 0.8 mm window separation. The cell was filled with dry DCM. Desorption of the sensitizer into solution over the course of an experiment was insignificant.

TRIR Spectrometer. The pump−probe broadband IR spectrometer has been previously described in detail.[13] Generation of probe light near 6 μm is accomplished by difference frequency mixing of two 10 Hz amplified synch-pumped dye laser pulses. The first dye laser uses LDS 751 in MeOH and no birefringent plates to produce broadband 25 μJ, 20 ps pulses at 750 nm. The pulses are amplified to 125 μJ in a two-stage dye amplifier (LDS 751) pumped with 3 mJ of Nd:YAG second harmonic pulses. The second dye laser uses a mixture of Rhodamine 640 (0.3 mmol/L) and Oxazine 720 (0.2 mmol/L) in MeOH and a three-plate birefringent filter to produce 20 μJ, 20 ps pulses at 655 nm, again amplified in a two-stage dye amplifier (LDS 698) to 150 μJ. Difference frequency mixing of the two synchronous dye pulses in a $AgGaS_2$ crystal (2 mm thick, 72°) produces ~25 cm^{-1} fwhm probe pulses tunable over the range of 1600−1800 cm^{-1}. The probe beam is split to provide parallel sample and reference beams of approximately 1 mm diameter at the sample.

Two methods of detection were used to analyze the intensity and spectral content of the light transmitted by the sample. In the first method, the transmitted probe beams are independently upconverted with two 50 μJ, 1.06 μm pulses in a second $AgGaS_2$ crystal (2 mm thick, 50°). The upconverted pulses contain the frequency-dependent transmission information of the IR probe but shifted to approximately 900 nm. The pulses are dispersed onto a 384 × 578 pixel CCD by a 0.22 m double monochromator using 1200 groove/mm holographic gratings. Alternatively, direct detection of the IR probe light was achieved by dispersing the two probe beams onto a 256 × 256 pixel HgCdTe (MCT) array detector via a 0.20 m single monochromator with a 70 groove/mm ruled grating. Due to the limited angular acceptance of the $AgGaS_2$ crystal, we could only achieve a useable probe bandwidth of ~25 cm^{-1} fwhm. Thus the spectral data are collected in several steps, overlapping successive probe regions by about 10 cm^{-1}.

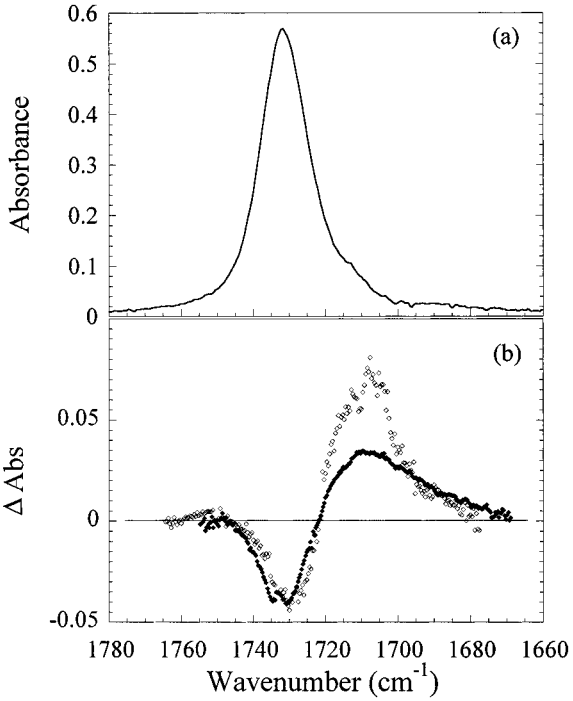

Figure 1. (a) Ground-state FTIR absorption spectrum of $[Ru(dceb)(bpy)_2]^{2+}$ in dichloromethane (DCM). (b) IR difference spectra for $[Ru(dceb)(bpy)_2]^{2+}$ in DCM 35 ps after visible excitation at 532 nm. The filled data points were collected using upconversion of the 6 μm probe light into the visible region for CCD array detection. The open data points were obtained via direct IR detection using a HgCdTe array. Other details are given in the text.

The 532 nm pump beam was ~2 mm in diameter at the sample and consisted of 800 μJ, 30 ps fwhm pulses. Pump−probe delay was computer controlled by an optical delay stage with 1 μm resolution in the pump line. The instrumental response function was measured from the single-sided cross-correlation of the IR probe with the visible pump pulse impinging on a Si wafer as described earlier.[13] Transient difference spectra are calculated as the logarithm of the average normalized transmission with the pump pulse blocked (typically 2000 shots) divided by the average normalized transmission with the pump on.[13]

Results and Discussion

The FTIR ground-state spectrum of $[Ru(dceb)(bpy)_2]^{2+}$ in DCM shown in Figure 1a displays an intense absorption band at 1731 cm^{-1} attributed to the ester C═O stretching mode. Figure 1b displays the infrared absorbance difference spectrum 35 ps after the visible excitation pulse. The bleach of the ground-state absorption band is readily apparent as is a new absorption shifted ~24 cm^{-1} to lower energy. These features appear within the time resolution of the instrument (~30 ps)

TABLE 1: Ester ν(C═O) Stretching Frequencies in the Electronic Ground State and MLCT Excited State with Frequency Shifts $\Delta\nu$

sample	FTIR Abs[a]	detector	bleach max[b]	abs max[b]	$\Delta\nu$, cm^{-1}
$[Ru(dceb)(bpy)_2]^{2+}$ in DCM	1731	CCD	1731	1709	−22
$[Ru(dceb)(bpy)_2]^{2+}$ in DCM		MCT	1731	1707	−24
$[Ru(dceb)(dmb)_2]^{2+}$ in DCM	1730	CCD	1734	1707	−27
$[Ru(dceb)(bpy)_2]^{2+}/ZrO_2$	1725	MCT	1728	1692	−36
$[Ru(dceb)(bpy)_2]^{2+}/TiO_2$	1726				

[a] Error ±1 cm^{-1}. [b] Error ±3 cm^{-1}.

and remain for at least 4 ns, consistent with subpicosecond $S_1 \rightarrow T_1$ intersystem crossing and submicrosecond $T_1 \rightarrow S_0$ excited-state relaxation as is characteristic for this class of MLCT compounds.[7,14] The results are in agreement with those recently obtained with 20 ns resolution by step-scan FTIR for the same molecule in acetonitrile.[5] To confirm whether related MLCT compounds exhibit similar behavior, we examined $[Ru(dceb)(dmb)_2]^{2+}$ in DCM. Spectra obtained for this sensitizer are nearly identical with $[Ru(dceb)(bpy)_2]^{2+}$, except for an additional transient absorption at 1620 cm^{-1}, which overlaps a ground-state feature and displays increased intensity but little or no frequency shift in the excited state. This transient is perhaps attributable to an increased dipole moment associated with structural changes in the bipyridine C−C ring stretching mode.

One common method of attachment of ruthenium polypyridyl derivatives to TiO_2 involves dehydrative covalent bonding of bipyridyl carboxylic acids to the oxide surface.[15b] However, carboxylic acids can form hydrogen-bonded dimers in solution, leading to complicated IR spectra having two or more peaks in the C═O region. The compounds in this study with the ethyl ester ligand (dceb) give a single C═O absorption and also bind tenaciously to ZrO_2 and TiO_2, presumably through the loss of the ethoxy group. The exact nature of the surface linkage is unknown, and several structures (**A**−**D**) are possible.[15b] Only one linkage (**A**) has two inequivalent carbon−oxygen bonds and is expected to display the higher energy asymmetric stretch. The small ≈ 5 cm^{-1} shift in ν(C═O) upon binding (see Table 1) indicates a minor perturbation of electronic structure by the metal oxide substrates and suggests that the binding mode is as depicted in **A**.

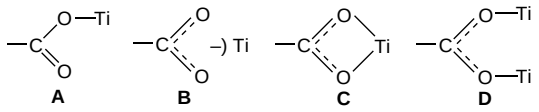

Since our intention was to use TRIR techniques to probe the electronic nature of the sensitizer/semiconductor interface, we first examined ZrO_2, which has similar surface and optical properties to TiO_2 but whose conduction band is approximately 1 eV higher in energy than that of TiO_2.[16] It is believed that the ZrO_2 conduction band lies significantly above the sensitizer excited-state oxidation potential, preventing electron transfer.[17] In this way we hoped to study the nature of the surface-anchored excited state in the absence of electron injection, in which case the excited-state electron density and TRIR spectra are expected to closely resemble those in solution. In fact, the TRIR spectrum of $[Ru(dceb)(bpy)_2]^{2+}/ZrO_2$ shown in Figure 2 displays bleach and absorption transients very similar to those in the solution experiment (see Figure 1b), although the peak separation increased to approximately 36 cm^{-1} and the absorption band is broadened. These results are summarized in Table 1.

$[Ru(dceb)(bpy)_2]^{2+}$ was also anchored to nanocrystalline TiO_2 films in order to directly measure the rate of electron injection. On the basis of an estimated 1 ns injection time constant from

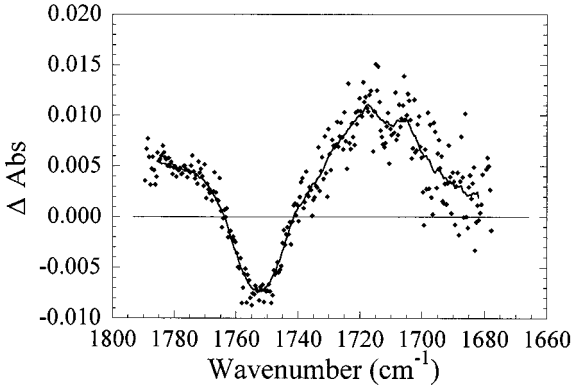

Figure 2. IR difference spectrum for $[Ru(dceb)(bpy)_2]^{2+}$ anchored to a ZrO_2 thin film in contact with dichloromethane. Detection is via a HgCdTe array 35 ps after 532 nm excitation. The solid line is a multipoint smoothed fit to guide the eye.

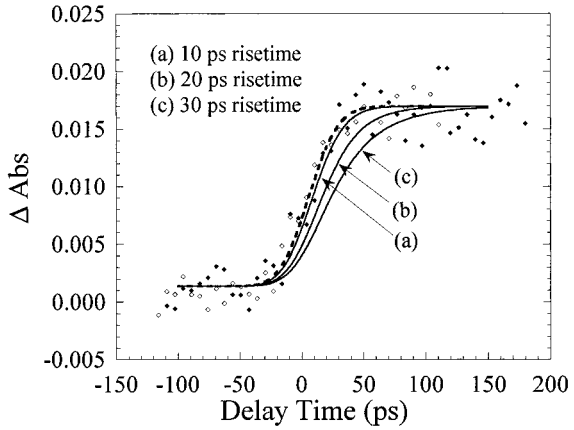

Figure 3. Absorbance difference integrated from 1640 to 1660 cm^{-1} as a function of probe delay time for Si in air (open symbols, relative ΔAbs) and $[Ru(dceb)(bpy)_2]^{2+}$ anchored to TiO_2 (filled symbols, absolute ΔAbs). Pump energy (at 532 nm) was reduced from 800 to 15 μJ for Si to produce a similar maximum absorbance change and prevent absorbance saturation. The dashed line is a nonlinear least-squares fit to the Si pump−probe cross-correlation. The solid lines are the responses expected for first-order growth time constants convoluted with the cross-correlation function.

TRPL measurements[1e] for the related sensitizer $[Ru(4,4'-(COOH)_2\text{-}2,2'\text{-bipyridine})(bpy)_2]^{2+}$, we expected to observe an initial shift in ν(C═O) to lower energy (as found for $[Ru(dceb)(bpy)_2]^{2+}/ZrO_2$) followed by nanosecond relaxation as the electrons are transferred to TiO_2. However, no bleach or shift of the ground-state FTIR absorbance was observed. One possibility is that the C═O absorbance change on going from Ru^{II} to Ru^{III} upon electron injection is smaller than the 0.002 OD detection limit. We note that in the step-scan FTIR experiment of Chen et al., when $[Ru(dceb)(bpy)_2]^{2+}$ was photolyzed in the presence of the electron acceptor methylviologen, ΔAbs was approximately $^1/_5$ of the excited-state absorbance change.[5] Instead, a broad positive absorption feature (ΔAbs ≈ 0.02) appears across the 1600−1800 cm^{-1} region with no apparent relaxation on the nanosecond time scale. On the basis of previous spectroscopic studies of both electrochemically and thermally reduced TiO_2,[18] this attenuation (absorption and/or reflection) arises from electrons in the TiO_2.[19] We note that no measurable signal is observed when unsensitized TiO_2 is used as the sample, indicating that two-photon or impurity absorption of the 532 nm excitation by TiO_2 is negligible. Figure 3 displays the growth of the attenuation for a $[Ru(dceb)(bpy)_2]^{2+}/TiO_2$ sample, integrated over 1640−1660 cm^{-1}, as a function of time. Also shown for comparison is the normalized response of a Si wafer in the same region also excited at 532

nm. The transient signal in Si is attributed to the instantaneous generation of free carriers upon excitation and gives the integrated cross-correlation of the pump and probe pulses. The similar shape of the $[Ru(dceb)(bpy)_2]^{2+}/TiO_2$ response indicates that the appearance of electrons in TiO_2 occurs within the resolution of our apparatus. Convolution of a slower response allows a conservative 20 ps upper limit to be placed on the electron injection time constant. While it would be ideal to have higher time resolution, even this upper limit allows us to calculate a minimum injection quantum yield, ϕ_{inj}, based on competition between electron injection, k_{inj}, and sensitizer excited-state decay, k_{D^*}. The excited state decay rate is assumed to be similar to that reported for the nearly identical compound $[Ru(dceb)(dmb)(bpy)]^{2+}$.[20]

$$\phi_{inj} = \frac{k_{inj}}{k_{inj} + k_{D^*}} = \frac{5.0 \times 10^{10}\ s^{-1}}{5.0 \times 10^{10}\ s^{-1} + 1.3 \times 10^{6}\ s^{-1}} > 0.99$$

This result is encouraging in that it suggests that very short-lived sensitizers (i.e., $\tau = 1-10$ ns) should give high injection yields, provided that the interfacial energetics are similar. We are currently examining the TRIR response of $Ru(dcb)_2(NCS)_2/TiO_2$ using subpicosecond probe and excitation pulses, in hopes to more precisely measure the electron injection rate(s) for these types of sensitizers. Preliminary results indicate a <1 ps initial injection with a possible longer component, in qualitative agreement with the visible transient absorption experiment.[6]

It is interesting to compare the data quality obtained by the two different detection methods. While the IR absorption difference spectra shown in Figure 1b are qualitatively very similar, the data obtained by direct detection with the MCT array has a lower S/N ratio. The advantage of CCD detection lies in its inherently low background noise, typically less than 30 counts per pixel. With appropriate background subtraction, baseline noise levels of ± 0.002 OD occur for an average of 4000 laser shots. Background noise, large dark counts and thermal fluctuations in the MCT camera (at 77 K) limit the noise level to ± 0.005 OD. While CCD detection requires inefficient nonlinear conversion of the IR probe light into the visible, the low CCD background noise results in a respectable S/N level.

Conclusions

We have developed a direct IR transient absorption method for measuring rates of interfacial electron transfer in sensitized semiconductor systems. This approach is particularly advantageous in that with proper selection of probe wavelength, it is sensitive to only the transfer of electrons into the semiconductor and not to interference by sensitizer excited-state absorption changes. Analysis of the signal growth allows a lower limit to be placed on the rate of electron injection for $[Ru(dceb)(bpy)_2]^{2+}/TiO_2$, $k > 5.0 \times 10^{10}\ s^{-1}$. These results show that high interfacial electron injection yields can be achieved for this class of sensitizers, as well as those with shorter lifetimes, leading to efficient photovoltaic devices.

References and Notes

(1) (a) Nakashima, N.; Yoshihara, K.; Willig, F. *Chem. Phys.* **1980**, *73*, 3553. (b) Nazeeruddin, M. K.; Liska, P.; Moser, J.; Vlachopoulos, N.; Grätzel, M. *Helv. Chim. Acta* **1990**, *73*, 1788. (c) Vinodogopal, K.; Hua, X.; Dahlgren, R. L.; Lappin, A. G.; Patterson, L. K.; Kamat, P. V. *J. Phys. Chem.* **1995**, *99*, 10883. (d) Hashimoto, K.; Hiramoto, M.; Lever, A.; Sakata, T. *J. Phys. Chem.* **1988**, *92*, 1016. (e) Heimer, T. A.; Meyer, G. J. *J. Lumin.* **1996**, *70*, 468.

(2) (a) O'Regan, B.; Moser, J.; Anderson, M.; Grätzel, M. *J. Phys. Chem.* **1990**, *94*, 8720. (b) Heimer, T. A.; Meyer, G. J. *Nanostructured Materials in Electrochemistry;* Meyer, G. J., Searson, P. C., Eds.; The Electrochemical Society: Pennington, NJ, 1995. (c) Kamat, P. V.; Bedja, I.; Hotchandani, S.; Patterson, L. K. *J. Phys. Chem.* **1996**, *100*, 4900.

(3) (a) Bignozzi, C. A.; Argazzi, R.; Schoonover, J. R.; Gordon, K. C.; Dyer, R. B.; Scandola, F. *Inorg. Chem.* **1992**, *31*, 5260. (b) Schoonover, J. R.; Gordon, K. C.; Argazzi, R.; Woodruff, W. H.; Peterson, K. A.; Bignozzi, C. A.; Dyer, R. B.; Meyer, T. J. *J. Am. Chem. Soc.* **1993**, *115*, 10996.

(4) (a) Dougherty, T. P.; Heilweil, E. J. *Chem. Phys. Lett.* **1994**, *227*, 19. (b) Dougherty, T. P.; Heilweil, E. J. *J. Chem. Phys.* **1994**, *100*, 4006. (c) Dougherty, T. P.; Grubbs, W. T.; Heilweil, E. J. *J. Phys. Chem.* **1994**, *98*, 9396.

(5) Chen, P.; Omberg, K. M.; Kavaliunas, D. A.; Treadway, J. A.; Palmer, R. A.; Meyer, T. J. *Inorg. Chem.* **1997**, *36*, 954.

(6) Tachibana, Y.; Moser, J. E.; Grätzel, M.; Klug, D. R.; Durrant, J. R. *J. Phys. Chem.* **1996**, *100*, 20056.

(7) Damrauer, N. H.; Cerullo, G.; Yeh, A.; Boussie, T. R.; Shank, C. V.; McCusker, J. K. *Science* **1997**, *275*, 54.

(8) Fessenden, R. W.; Kamat, P. V. *J. Phys. Chem.* **1995**, *99*, 12902.

(9) *Disclaimer:* Certain commercial equipment, instruments, or materials are identified in this paper in order to adequately specify the experimental procedure. In no case does such identification imply recommendation or endorsement by the National Institute of Standards and Technology, nor does it imply that the materials or equipment identified are necessarily the best available for the purpose.

(10) Maerker, G.; Case, F. H. *J. Am. Chem. Soc.* **1958**, *80*, 2745.

(11) Sullivan, B. P.; Salmon, D. J.; Meyer, T. J. *Inorg. Chem.* **1978**, *17*, 3334.

(12) Heimer, T. H.; D'Arcagelis, S. T.; Farzad, F.; Stipkala, J. M.; Meyer, G. J. *Inorg. Chem.* **1996,** *35*, 5319.

(13) Heilweil, E. J.; Cavanagh, R. R.; Stephenson, J. C. *Chem. Phys. Lett.* **1987**, *134*, 181. Dougherty, T. P.; Heilweil, E. J. *Opt. Lett.* **1994**, *19*, 129.

(14) Meyer, T. J. *Pure Appl. Chem.* **1986**, *58*, 1193.

(15) (a) Grünwald, R.; Tributsch, H. *J. Phys. Chem. B* **1997**, *101*, 2564. (b) Argazzi, R.; Bignozzi, C. A.; Heimer, T. A.; Castellano, F. N.; Meyer, G. J. *Inorg. Chem.* **1994**, *33*, 5741.

(16) (a) Kung, H. H.; Jarrett, H. S.; Sleight, A. W.; Ferretti, A. *J. Appl. Phys.* **1977**, *48*, 2463. (b) Clechet, P.; Martin, J.; Oliver, R.; Vallouy, C. *C. R. Acad. Sci. C* **1976**, *282*, 887.

(17) While good electrochemical data to locate the sensitizer excited-state energy level relative to the acceptor bands of TiO_2 and ZrO_2 in DCM do not exist, photoluminescent quenching measurements show that electron transfer from related sensitizers occurs to TiO_2 but not ZrO_2.[1e]

(18) (a) Cao, F.; Oskam, G.; Searson, P. C.; Stipkala, J. M.; Heimer, T. A.; Farzad, F.; Meyer, G. J. *J. Phys. Chem.* **1995**, *99*, 11974. (b) Von Hippel, A.; Kalnajs, J.; Westphal, W. B. *J. Phys. Chem. Solids* **1962**, *23*, 779.

(19) As pointed out by a reviewer, the IR experiment does not differentiate between types of electrons in TiO_2. They could be free carriers in the TiO_2 conduction band or trapped, for example, at Ti^{IV} sites as Ti^{III}.

(20) Strouse, G. F.; Anderson, P. A.; Schoonover, J. R.; Meyer, T. J.; Keene, F. R. *Inorg. Chem.* **1992**, *31*, 3004.